INSTITUT D'AERONOMIE SPATIALE DE BELGIQUE

3 - Avenue Circulaire
B - 1180 BRUXELLES

# AERONOMICA ACTA

## A - N° 161 - 1976

## STEADY STATE PLASMAPAUSE POSITIONS DEDUCED FROM McILWAIN'S ELECTRIC FIELD MODELS

by

J. LEMAIRE

BELGISCH INSTITUUT VOOR RUIMTE-AERONOMIE

3 - Ringlaan
B - 1180 BRUSSEL

## FOREWORD

The paper entitled "Steady state plasmapause positions deduced from McIlwain's electric field models" was presented at the "Physics of the Plasmapause" symposium, in Grenoble, 28 August - 3 September, 1975. This article will be published in Journal of Atmospheric and Terrestrial Physics.

## AVANT-PROPOS

L'article intitulé "Steady state plasmapause positions deduced from McIlwain's electric field models" a été présenté au symposium sur la "Physique de la Plasmapause" à Grenoble, 28 août - 3 septembre, 1975. Ce texte sera publié dans Journal of Atmospheric and Terrestrial Physics.

## VOORWOORD

Het werk "Steady state plasmapause positions deduced from McIlwain's electric field models" werd voorgedragen tijdens het symposium "Physics of the Plasmapause", in Grenoble, 28 augustus - 3 september 1975. De tekst zal gepubliceerd worden in Journal of Atmospheric and Terrestrial Physics.

## VORWORT

Das Artikel "Steady state plasmapause positions deduced from McIlwain's electric field models" wurde zum "Physics of the Plasmapause" Symposium in Grenoble (28 August - 3 September, 1975) vorgestellt. Dieser Text wird in Journal of Atmospheric and Terrestrial Physics veroffendlicht.

# STEADY STATE PLASMAPAUSE POSITIONS DEDUCED FROM McILWAIN'S ELECTRIC FIELD MODELS

by

J. LEMAIRE

*Abstract*

It has recently been suggested that the plasmasphere of the Earth is peeled off near midnight (at L = 4.5 for $K_p$ = 1-2) by "Plasma Elements Interchange Motion" driven by centrifugal or inertial forces. McIlwain's (1974) convection electric field model E3H with a variable scale factor f has been used to calculate different plasmapause positions and shapes. The new theoretical models obtained with $f \geqslant 1.2$ are in agreement with observations of whistlers and of the PROGNOZ satellites, for periods of very low geomagnetic activity (i.e. $K_p < 1$). Furthermore the numerical models corresponding to $f \leqslant 0.7$ fit qualitatively the observations of the plasmasphere and plasmapause when the geomagnetic activity has a higher constant level (i.e. $2 < K_p < 4$). A tentative relation between f and $K_p$ is deduced.

*Résumé*

Récemment il a été suggéré que la plasmasphère de la Terre est formée dans le secteur de temps local voisin de minuit (en L = 4,5 pour $K_p$ = 1-2) par le mécanisme d'échange des éléments de plasma dû à l'action des forces centrifuges ou d'inertie. Le champ électrique E3H de McIlwain (1974) avec facteur d'échelle variable (f) a été utilisé pour calculer différentes positions et formes de la plasmapause. Les nouveaux modèles théoriques obtenus pour $f \geqslant 1.2$ sont en accord avec les observations des "Siffleurs atmosphériques" ainsi qu'avec les observations directes des satellites PROGNOZ en périodes de très faible activité géomagnétique (c.à.d. : $K_p < 1$). D'autre part les modèles correspondant à $f \leqslant 0.7$ concordent avec les observations de la plasmasphère et de la plasmapause lorsque l'activité géomagnétique se maintient à un niveau plus élevé (c.à.d. : $2 < K_p < 4$). Une relation entre f et $K_p$ a été déduite.

*Samenvatting*

Onlangs werd voorgesteld dat de plasmasfeer van de aarde in het gebied overeenstemmend met een plaatselijke tijd nabij middernacht (L = 4.5 voor $K_p$ = 1-2) gevormd wordt door het uitwisselingsmechanisme van de plasmaelementen onder invloed van de centrifugale of inertie krachten. Het convectie electrisch veldmodel E3H van McIlwain (1974) met een veranderlijke schaalfactor f werd gebruikt om de plaats en vorm van de plasmapauze te berekenen voor verschillende gevallen. De nieuwe theoretische modellen bekomen voor $f \geqslant 1.2$ zijn in overeenstemming met fluiter-waarnemingen en de metingen met behulp van de PROGNOZ satellieten voor perioden met zeer kleine geomagnetische activiteit ($K_p < 1$). De numerieke modellen voor $f \leqslant 0.7$ stemmen qualitatief goed overeen met de waarnemingen van de plasmasfeer en de plasmapauze wanneer de geomagnetische activiteit konstant is en belangrijker, nl. $2 < K_p < 4$. Een betrekking tussen f en $K_p$ werd afgeleid.

*Zusammenfassung*

Das elektrische Feldmodell E3H von McIlwain (1974) wurde für verschiedene Skalenfactoren, f, angewändet um die Plasmapauzelagen zu berechnen. Die neuen theoretischen Modelle mit $f \geqslant 1.2$ sind in gutter Übereinstimmung mit die Beobachtungen für geringe geomagnetische Aktivität ($K_p < 1$). Die numerische Modelle mit $f \leqslant 0.7$ entsprechen auch die Beobachtungen für höhere geomagnetische Aktivitäten ($2 < K_p < 4$). Eine Relation zwischen f und $K_p$ is abgezogen worden.

## *1. FORMATION OF THE PLASMAPAUSE*

According to a recent theory the plasmapause is peeled off in the post-midnight sector by *plasma elements interchange motion** driven by centrifugal forces beyond a *"Roche-limit surface"* (Lemaire, 1974). The Roche-limit is defined as the surface beyond which the gravitational force and the centrifugal force** balance each other in the direction parallel to the local magnetic field $\vec{B}$. The solid line in Figure 1 running from dawn to dusk across the equatorial plane of the magnetosphere shows the section of the Roche-limit surface when the azimuthal components of the electric drift velocity ($\vec{E} \times \vec{B}/B^2$) and the local angular velocity ($\vec{\Omega}$) of the thermal plasma (< 1 eV) are determined from the E3H and M2 electric and magnetic field models proposed by McIlwain (1974).

Field aligned hydrostatic distributions of the exospheric plasma are convectively unstable for all magnetic field lines crossing this surface; outside the Roche-limit any plasma inhomogeneity (volume element with a higher density than the background medium) tends to move away from the Earth's surface along the magnetic field line, and, eventually across electric equipotential surfaces ($\varphi_E$ = cst) from one magnetic field line to another. However such cross-$\phi_E$ interchange motions of detached plasma elements are only possible when, $\Sigma_p$, the integrated Pedersen conductivity is significantly reduced below its commonly assumed infinite value***. As a consequence of the reduction of electric conductivity in the night-

---

* *Plasma elements interchange motion* is sometimes called *"Magnetic flux tubes interchange motion"* in the MHD or field-frozen-in approximation. (Sonnerup and Laird, 1963).

** The centrifugal force density ($\rho u^2/R_c$) acting on a plasma rotating with a uniform angular speed $\vec{\Omega}$ is equal to the inertial force density $\rho d\vec{u}/dt$ or $\rho(\vec{u}\vec{\nabla})\vec{u}$ since $\vec{u} = \vec{\Omega} \times \vec{R}_c$). When the drift velocity $\vec{u} = \vec{E} \times \vec{B}/B^2$ is determined by the corotation electric field, the equatorial radius of curvature, $R_c$, is equal to R, the radial distance. This is also true for McIlwain's convection electric field distribution, at least in the post-midnight sector where the equipotential lines are nearly parallel to concentric circles in the plasmasphere and in the plasmatrough.

*** In the MHD or field-frozen-in approximation $\Sigma_p = \infty$. The maximum velocity of interchange motion is zero since ($v_{MAX} \propto \Sigma_p^{-1}$ the radial velocity of a plasma element in an external force is limited by the rate of dissipation of the potential energy by Joule heating in the E-region.

side and high latitude E-region, $v_{MAX}$, the maximum velocity of cross-$\phi_E$ interchange motion is significantly enhanced. Due to the dominant centrifugal (or inertial) forces at $L \geqslant 4.5$, $v_{MAX}$ reaches values of the order of 0.5 L/hour near 0100 LT at the place of deepest penetration of the Roche-limit surface, i.e. where the plasmasphere is peeled off, and, where the plasmapause is formed (Lemaire, 1974, 1975).

If the electric field distribution in the magnetosphere does not change for at least 24 hours, the plasmasphere (inner shaded region in Figure 1) will become bounded by a surface which approximately coincides with an equipotential tangent to the Roche-limit surface at its deepest penetration point.

In the plasmatrough region (unshaded in Figure 1) the magnetic flux tubes are filled up during the day hours by evaporation from the topside ionosphere, and, by Coulomb pitch angle scattering. The plasma contents of these flux tubes are convected toward the nightside magnetosphere beyond the Roche-limit surface.where enhanced interchange motion will transport the (partially) filled elements beyond the last closed equipotential into the outermost region of the magnetosphere (outer shaded region in Figure 1). Once it has penetrated into this region (which approximately corresponds to the plasmasheet) the thermal plasma invariably will be convected on an open magnetic flux tube of the polar cusp (or cleft) where finally it is released into the magnetosheath along the flanks of the magnetopause. The drawings in Figure 2 illustrates the evolution of a plasma element convecting from the dayside plasmatrough toward the polar cusp merging magnetic field lines. The outer edge of the plasmatrough is perhaps related to the substorm injection boundary introduced by McIlwain (1974) and Mauk and McIlwain (1974); it corresponds to the zero-energy- Alfvèn layer: i.e. the limit of the forbidden region for cold electrons and ions convecting earthward in the plasmasheet.

A more detailed description of the three regions illustrated in Figure 1 (plasmasphere, plasmatrough, and plasmasheet) is given elsewhere (see, Lemaire, 1975).

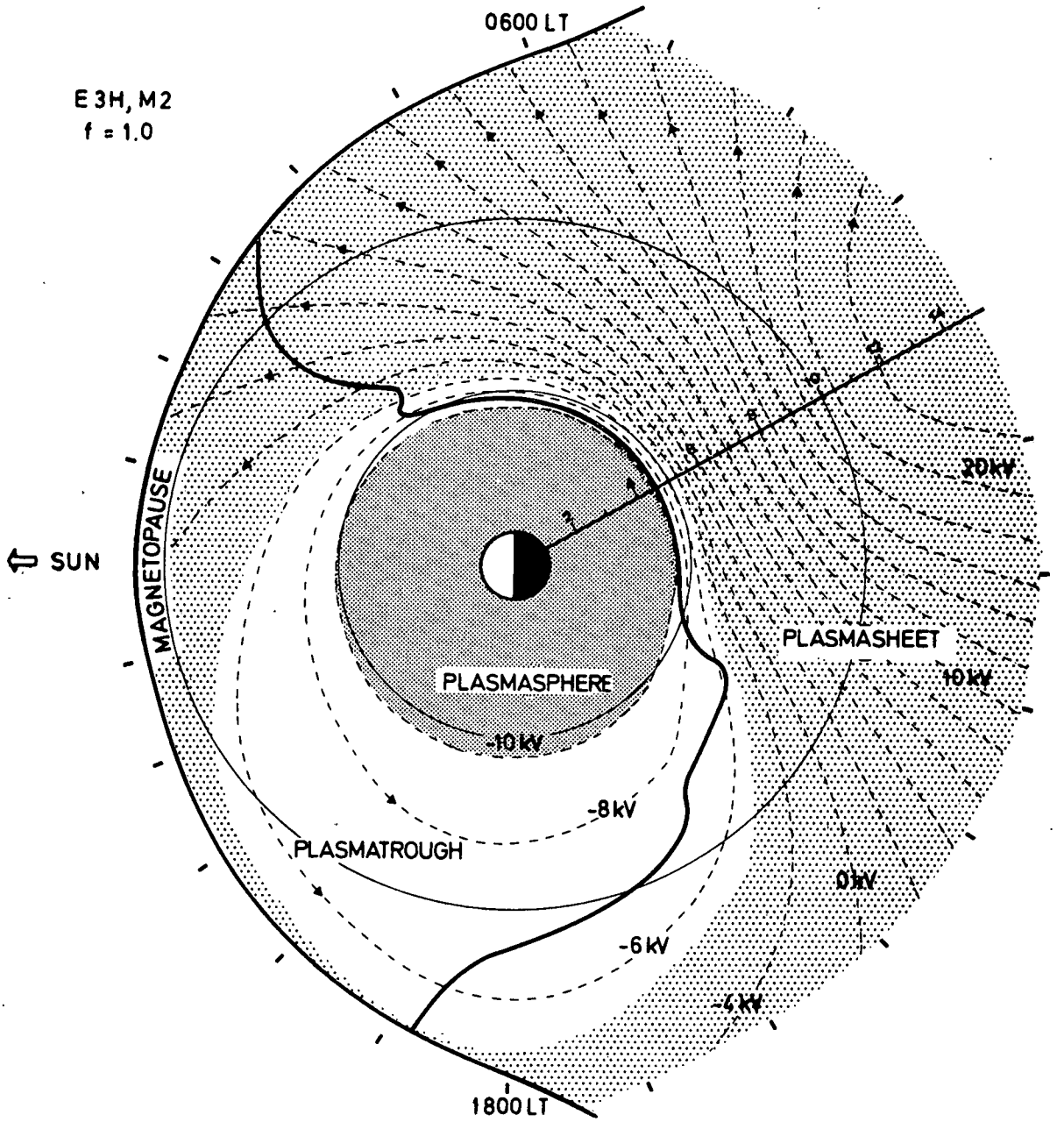


Fig. 1.- *The plasmapause for McIlwain's [1974] electric field model E3H (f=1)*; the dashed lines are the equatorial sections of the electrostatic potentials; the solid line accross the magnetosphere is the equatorial section of the Roche-limit surface where the gravitational and centrifugal forces balance each other along the magnetic field direction. The boundary of the inner shaded region is tangent to the Roche-limit surface near midnight; the inner boundary of the outer shaded region is the last closed electric equipotential surface, i.e. the Alfvèn layer for zero energy electrons and ions.

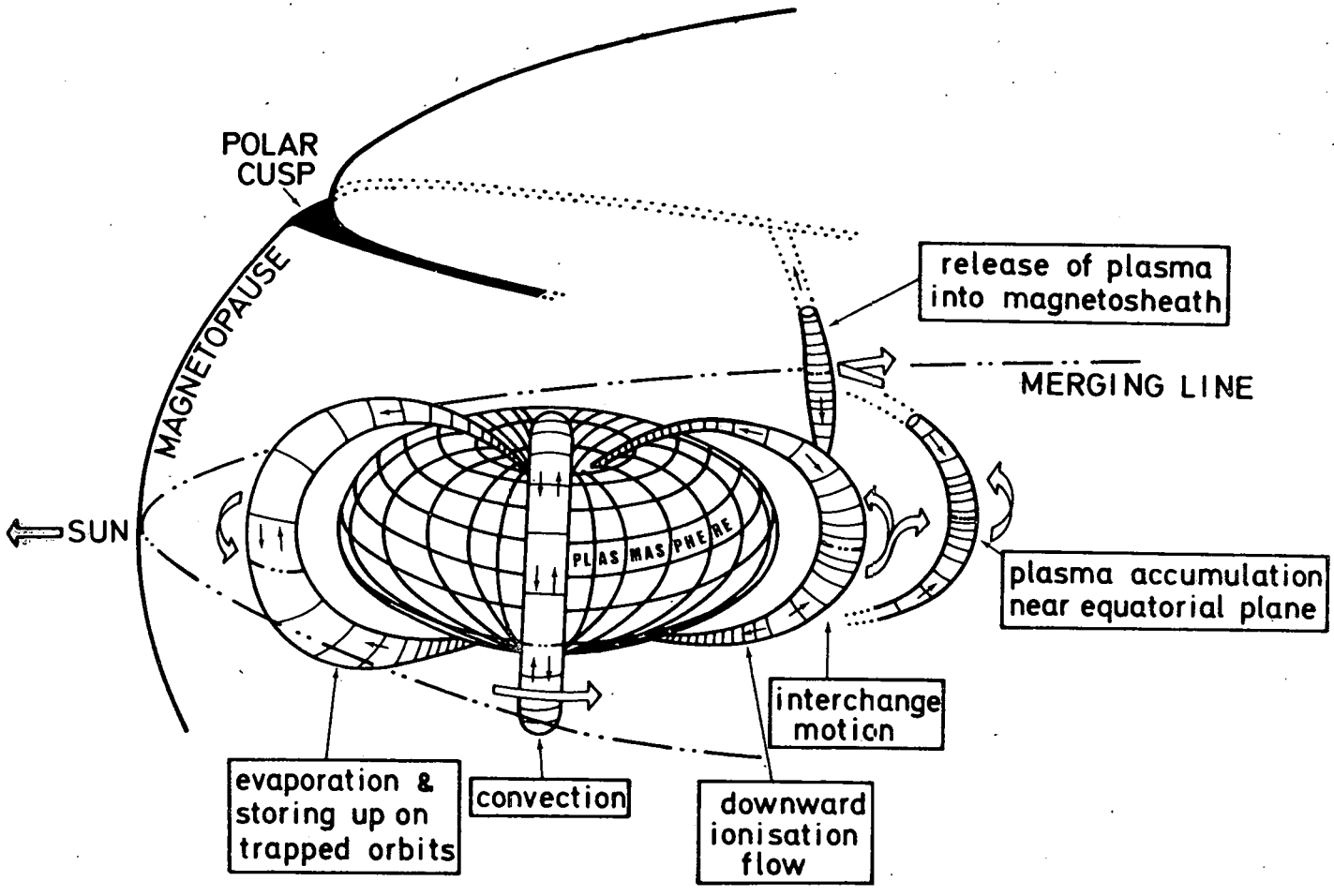


Fig. 2.- *Illustration of a field-aligned plasma element drifting in the plasmatrough.* Evaporation from the topside ionosphere and Coulomb pitch angle scattering in the dayside ion-exosphere concur to store cold charged particles on trapped orbits with high altitudes mirror points. The electric drift leads these particles around the plasmasphere toward the nightside region and beyond the Roche- limit surface. As a consequence of the reduction of the integrated Pedersen conductivity after sunset, interchange motion can transport plasma elements across equipotential surfaces at a significant rate. Therefore the cold trapped plasma accumulated near the equatorial plane moves outwardly into the region of "open" equipotentials, and, finally it reaches the magnetopause where the plasma is released from the magnetosphere along the merging polar cusp magnetic field lines.

## 2. *PLASMAPAUSE FOR DIFFERENT ELECTRIC FIELD MODELS*

From the previous description it appears that the position of the plasmapause is determined by the minimum radial distance of a Roche-limit surface i.e. by the convection velocity (in the midnight sector) which is a function of the magnetospheric electric field and magnetic field intensities.

In most of our model calculations we adopted McIlwain's (1972) magnetic model M2:

$$B(\gamma) = 6 - 24 \cos\varphi + 18 \cos^2\varphi/(1 + 1728/R^3) + 31000/R^3 \qquad (1)$$

where $\varphi$ is the local time angle (LT), and R is the radial distance in Earth radii. The lines of equal magnetic field intensity for the model M2 are shown by the solid curves in Figure 3. This model differs from Olson and Pfitzer (1974) model (abreviated version) shown by dashed lines in the lower part of Figure 3. The shaded areas correspond to the equatorial regions where the relative disagreement measured by $(B_{M2} - B_{O-P})/B_{M2}$ exceeds - 20% and + 20%. It can be seen that in the plasmasphere and plasmapause regions (i.e. $R < 5$-6) the M2 model used in the present paper is rather conservative and differs not too much from a dipole configuration.

The electric equipotentials(dasked lines in Figure 1) are determined by

$$\phi(kV) = 10 - 92 \left(\frac{B}{31000}\right)^{1/3} + \sum_{i=1}^{6} \sum_{j=1}^{20} A_{ij} \exp \{ - a_i (B - B_i)^2 - b_j [1 - \cos(\varphi - \varphi_j)] \} \qquad (2)$$

where the constants $B_i$ (in $\gamma$), $a_i = \ln 2/d_i^2$ (in $\gamma^{-2}$), $\varphi_j$ (in LT hours), $b_j = \ln 2/(1 - \cos C_j)$ and $A_{ij}$(in kV) can be deduced from Table 1 for the model E3H (taken from McIlwain, 1974). A similar expansion describes McIlwain's earlier model E3 (see, McIlwain, 1972).

Both electric field distributions E3 and E3H have been proposed for steady geomagnetic activity corresponding to $K_p$ = 1-2. Both models predict quite the same

TABLE 1.- Model E3H

| j | $A_{ij}$ | $A_{2j}$ | $A_{3j}$ | $A_{4j}$ | $A_{5j}$ | $A_{6j}$ | $\varphi_j$ | $C_j$ |
|---|---|---|---|---|---|---|---|---|
| 1 | 6.49 | 3.26 | 2.30 | 1.12 | - 0.24 | 0.17 | 4 | 2 |
| 2 | 1.37 | 0.83 | 0.38 | 0.48 | - 0.17 | 0.13 | 6 | 2 |
| 3 | 1.73 | 0.84 | 0.36 | 0.50 | - 0.26 | 0.08 | 8 | 2 |
| 4 | 0.69 | - 0.13 | - 0.31 | 0.16 | - 0.28 | - 0.03 | 10 | 2 |
| 5 | 0.90 | - 0.49 | - 0.53 | - 0.09 | - 0.41 | - 0.17 | 12 | 2 |
| 6 | 0.06 | - 1.04 | - 0.88 | - 0.37 | - 0.46 | - 0.26 | 14 | 2 |
| 7 | - 0.96 | - 1.78 | - 1.11 | - 0.64 | - 0.62 | - 0.38 | 16 | 2 |
| 8 | - 2.30 | - 1.78 | - 1.28 | - 0.53 | - 0.60 | - 0.32 | 18 | 2 |
| 9 | - 3.20 | - 2.13 | - 1.75 | - 0.89 | - 0.83 | - 0.43 | 20 | 2 |
| 10 | - 0.78 | - 1.09 | - 0.06 | - 0.63 | 0 | - 0.17 | 21 | 1 |
| 11 | 1.00 | - 1.10 | - 0.29 | - 0.49 | - 0.27 | - 0.19 | 22 | 1 |
| 12 | 0.59 | 0.07 | - 0.04 | 0.03 | - 0.16 | - 0.05 | 22.5 | 0.5 |
| 13 | 1.20 | 0.28 | 0.17 | 0.13 | - 0.20 | - 0.05 | 23 | 0.5 |
| 14 | 2.24 | 0.77 | 0.57 | 0.29 | - 0.29 | - 0.08 | 23.5 | 0.5 |
| 15 | 2.64 | 1.13 | 0.94 | 0.40 | - 0.23 | - 0.06 | 0 | 0.5 |
| 16 | 3.47 | 1.67 | 1.38 | 0.53 | - 0.22 | - 0.06 | 0.5 | 0.5 |
| 17 | 2.48 | 1.27 | 1.05 | 0.38 | - 0.12 | - 0.03 | 1 | 0.5 |
| 18 | 2.00 | 1.04 | 0.84 | 0.30 | - 0.08 | - 0.02 | 1.5 | 0.5 |
| 19 | 5.67 | 2.92 | 2.28 | 0.76 | - 0.13 | - 0.02 | 2 | 1 |
| 20 | 2.23 | 1.00 | 0.72 | 0.30 | - 0.03 | 0.06 | 3 | 1 |
| i | 1 | 2 | 3 | 4 | 5 | 6 | | |
| $B_i$ | 0 | 40 | 100 | 180 | 280 | 400 | | |
| $d_i$ | 30 | 50 | 70 | 90 | 110 | 130 | | |

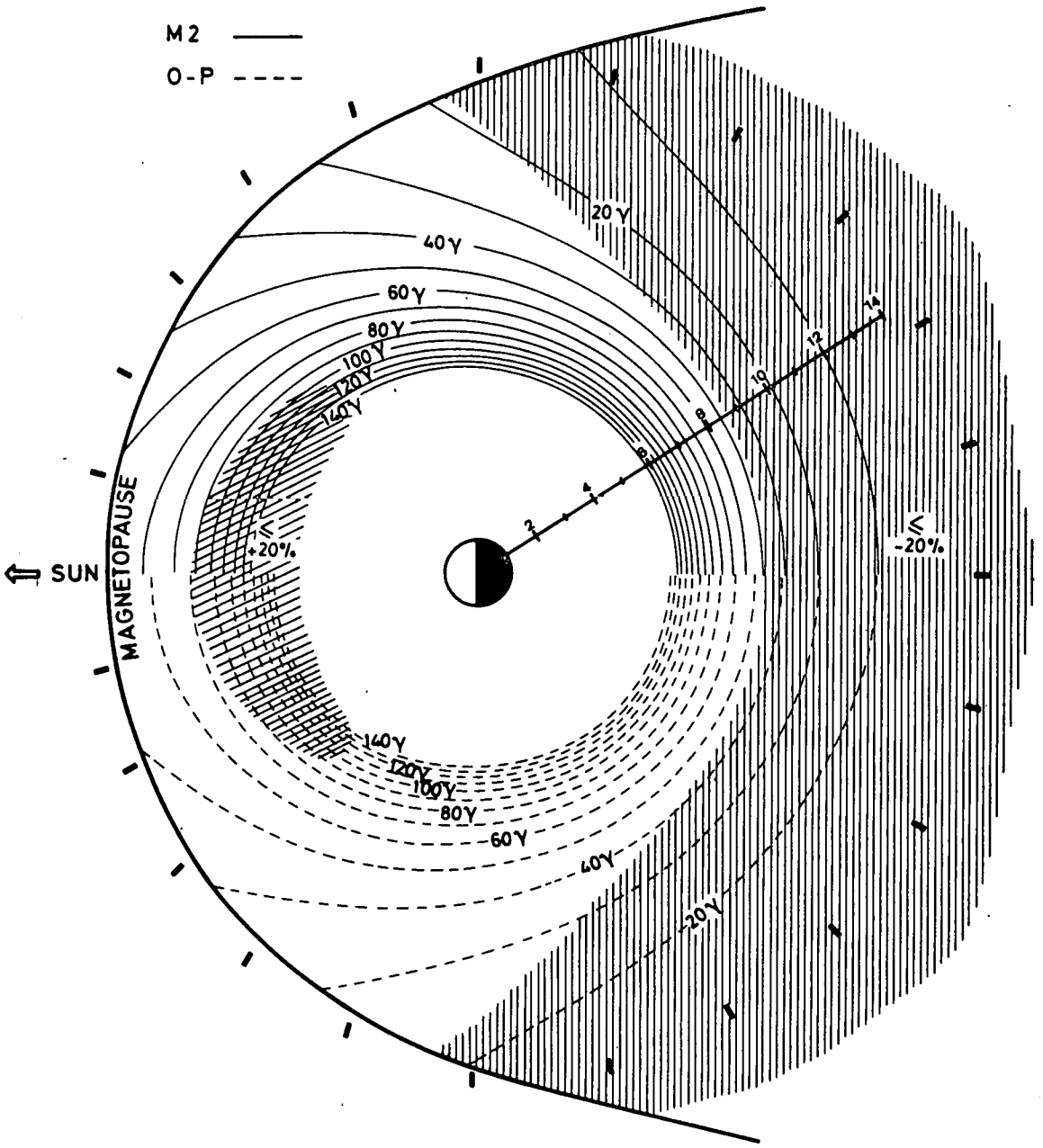


Fig. 3.- *Comparison of magnetic field models.* The solid curves (upper part) are isointensity lines of McIlwain's (1972) magnetic field model M2. The dasked curves (lower part) correspond to Olson and Pfitzer's (1974) model (abreviated version). The shaded zones indicate the areas where the relative difference of the magnetic field intensities $[(B_{M2} - B_{O-P})/B_{M2}]$ is larger than + 20% and - 20%.

plasmapause positions for nearly all local time angles except for 2000 LT $< \varphi <$ 2300 LT. The E3 model predicts a slightly more prominent bulge in this range of local times (compare Figure 1 and Lemaire's (1974) Figure 3).

To obtain better correspondance to $K_p$ values outside the range of $1 < K_p < 2$, McIlwain (1974) introduced a scale factor f such that a family of different electric field models can be derived by the conversion $B'_i = B_i/f^3$, $a'_i = a_i\ f^6$ and $A'_{ij} = A_{ij}/f$. The E3H model illustrated in Figure 1, actually corresponds to f = 1. For f smaller than 1 the convection electric field is enhanced, and, the dawn-dusk asymmetry of the closed equipotential surfaces is reinforced as can be seen by the dashed lines in Figure 4 for f = 0.70.

When f is larger than 1 the convection electric field decreases everywhere and the corotation electric field (second term in r.h.s. of eq. 2) prevails at larger radial distances, as illustrated by the more circular equipotential lines of Figure 5 obtained for f = 1.3. The equatorial section of the Roche-limit surface as well as the steady state plasmapause and the Alfvèn layer have been determined as described in the previous section. The new position of these boundaries are shown in Figures 4 and 5 for f = 0.7 and f = 1.3. The magnetopause boundaries in Figures 1, 4 and 5 are determined by

$$B(\gamma) = f_{MP}\,(16 - 35\cos\varphi + 12\cos^2\varphi) \qquad (3)$$

where $f_{MP}$ is a scale factor accounting qualitatively for the change in the magnetopause position with geomagnetic activity (Bridge *et al.*, 1965; Egidi *et al.*, 1970; Fairfield, 1971; Gringauz *et al.*, 1975); for $f_{MP}$ = 1, 0.7 and 1.3 the magnetopause distances at subsolar point are equal to 10.7 $R_E$, 8.7 $R_E$ and 12.2 $R_E$ respectively, as in Figures 1, 4 and 5.

A whole sequence of steady state plasmapause positions for successive values of f is shown in Figure 6 where the central shaded area corresponds to the plasmasphere for f = 1.

Finally, Figure 7 shows the theoretical position of the plasmapause as a function of the scale factor f, at 4 different LT angles.

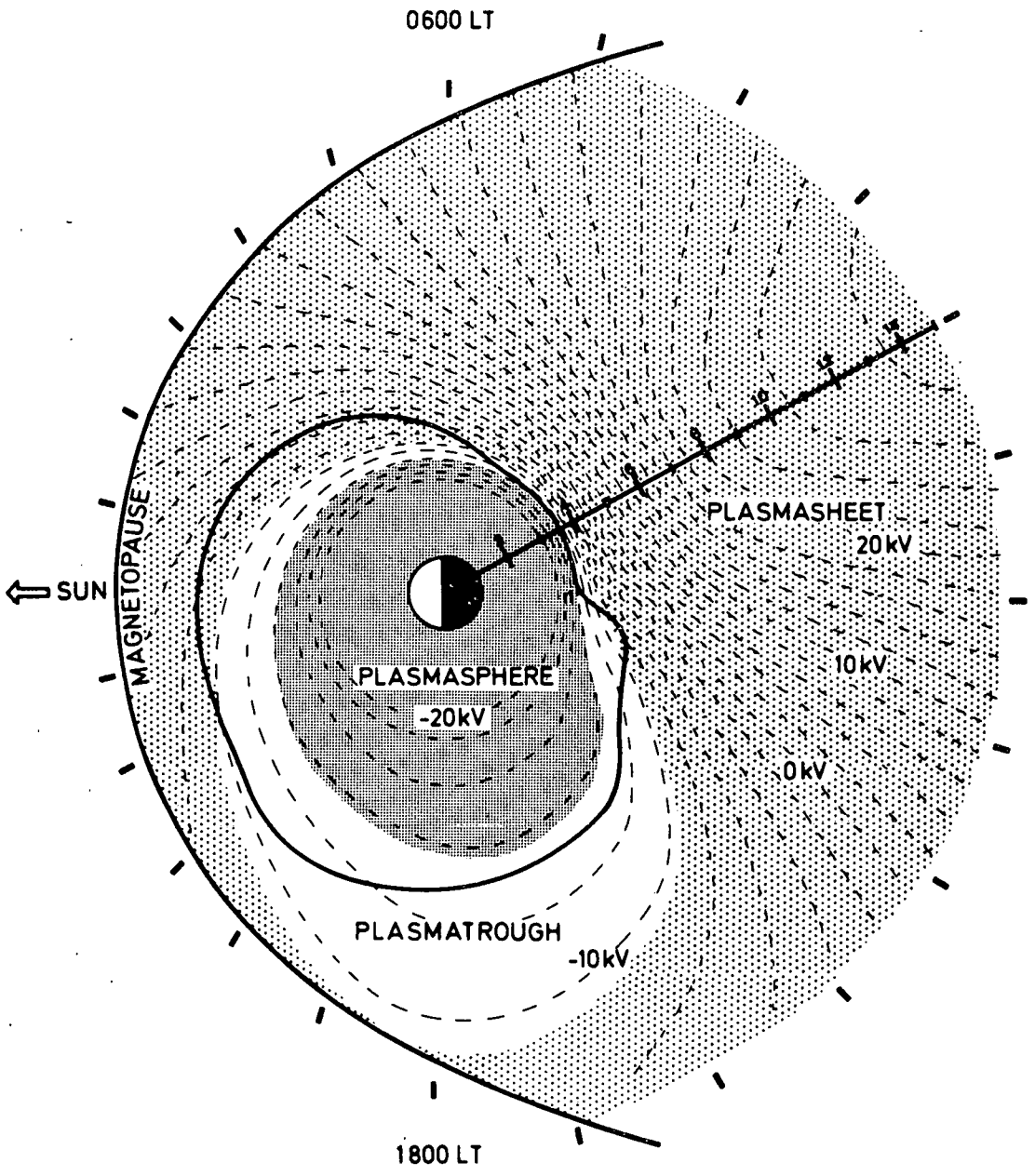


Fig. 4.- *The Plasmapause for McIlwain's (1974) electric field model E3H (f = 0.7).* (see and compare with figure 1). The dusk side bulge of the plasmapause is enhanced as during extended periods of moderate or high geomagnetic activity ($K_p > 2$).

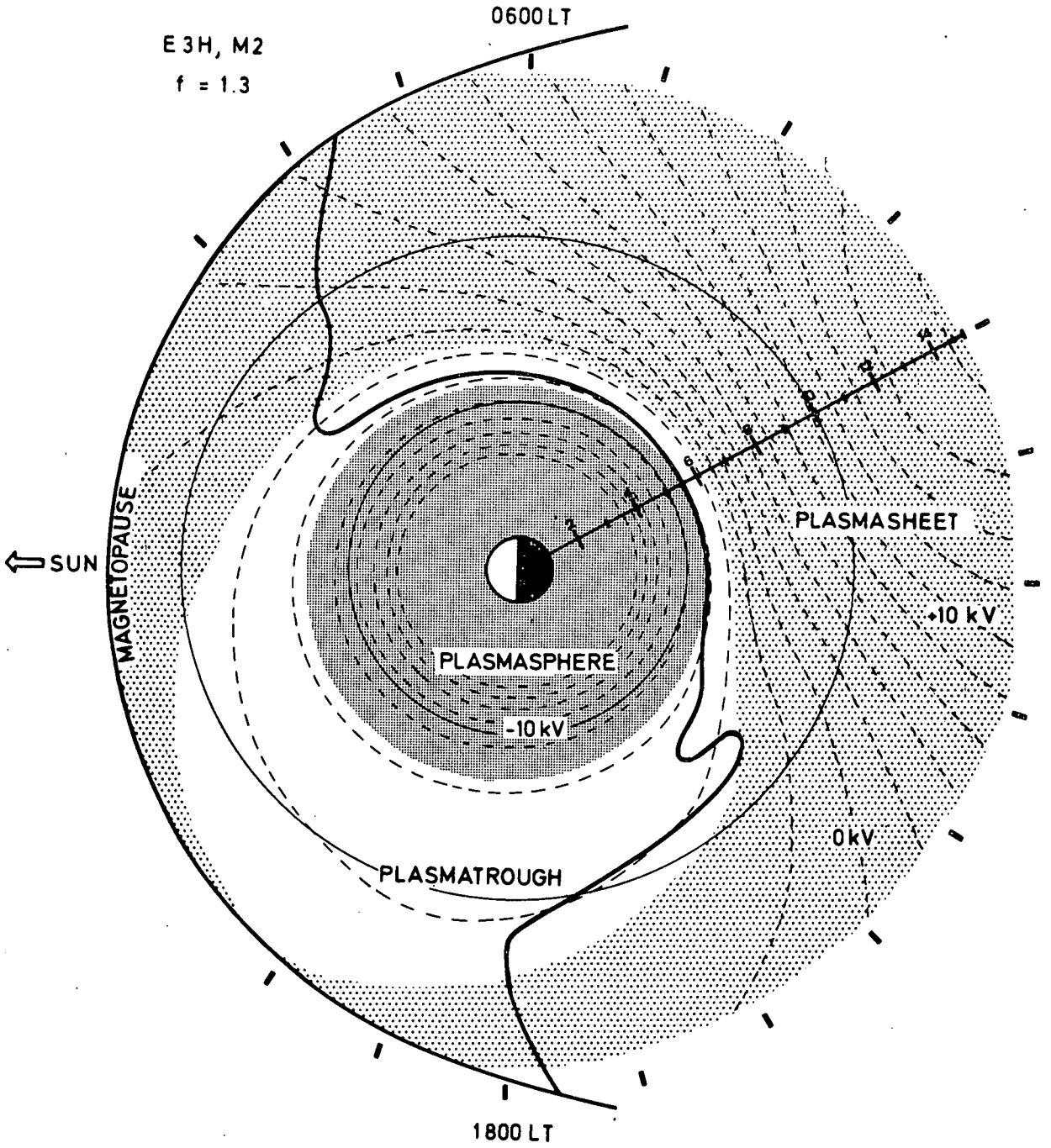


Fig. 5.- *The Plasmapause for McIlwain's (1974) electric field model E3H (f = 1.3).* (see and compare with figure 1). The plasmasphere and plasmapause extend at larger radial distances in the noon direction than in the midnight sector. A similar noon-midnight asymmetry is observed by whistlers and satellites during extended periods of very low geomagnetic activity (Kp < 1).

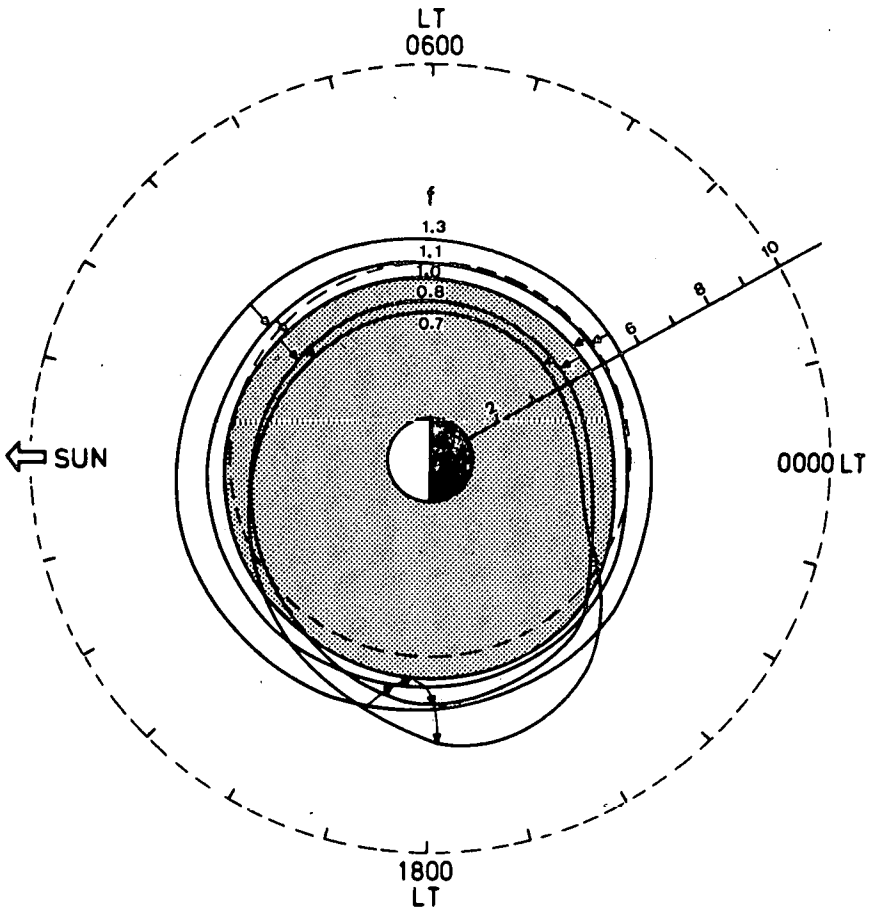


Fig. 6.- *Plasmapause position as a function of local time and as a function of the scale factor f of the E3H electric field model.* When f decreases from 1.3 to 0.7 the shape of the plasmapause changes from a large eccentric circle to a highly asymmetric "droplet" with a bulge in the 2000 LT direction. Similar deformations of the plasmasphere and plasmapause have been observed when Kp takes constant values from 0 to 4. The shaded area corresponds to the plasmasphere for f = 1.0.

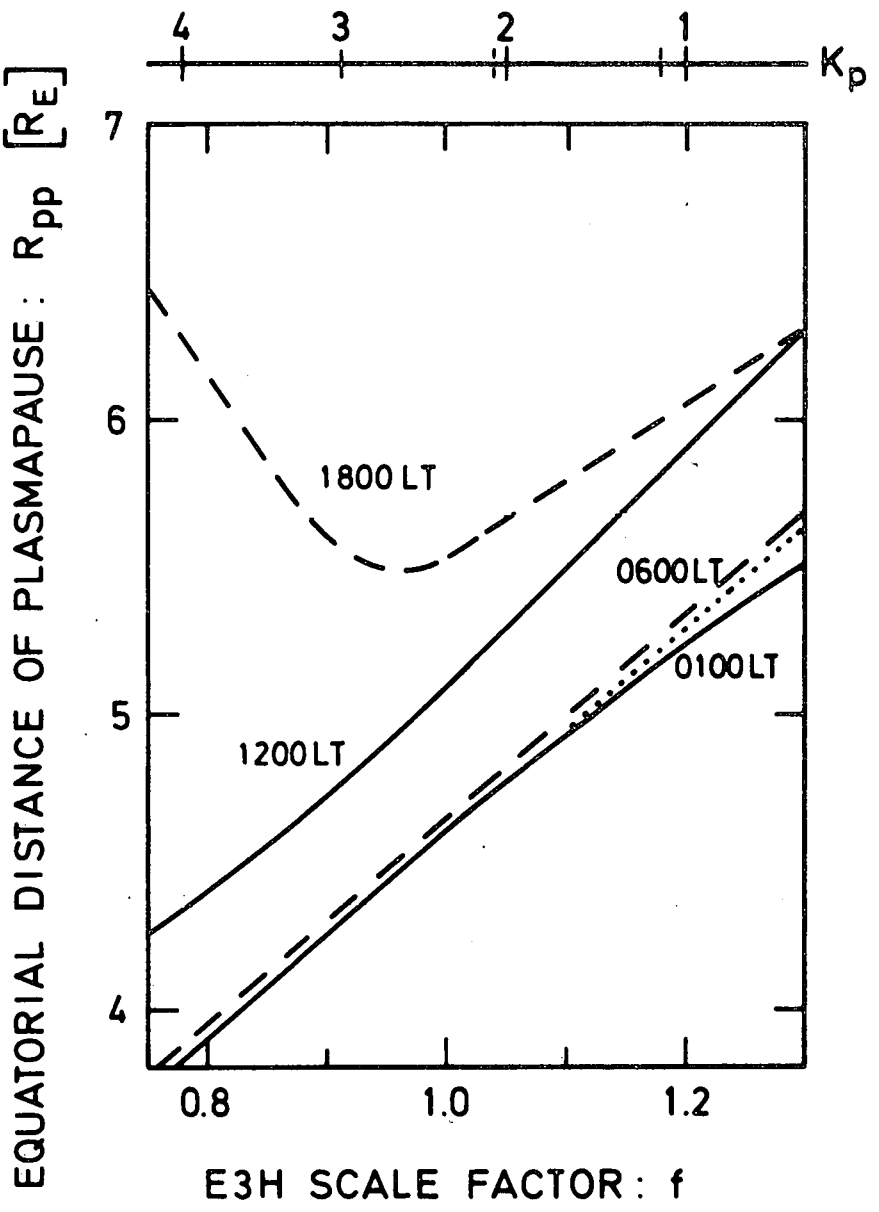


Fig. 7.- *The equatorial distances of the plasmapause at midnight, dawn, noon and dusk as a function of the scale factor f.* The noon-midnight asymmetry of the plasmapause increases when f increases. The dawn-dusk asymmetry increases when f decreases.

*3. DISCUSSION*

Let us consider with McIlwain (1974) that the sequence of E3H models obtained by changing the scale factor f corresponds to the large scale electric field distribution in the magnetosphere for different constant geomagnetic conditions i.e. for different values of the $K_p$ index. From the sequence of plasmapause positions and shapes illustrated in Figures 6 and 7 it can be concluded that larger (smaller) values of f are associated to smaller (larger) values of $K_p$. Indeed,

i) the observed plasmapause distance in the post-midnight sector decreases when $K_p$ increases,

$$L_{pp} = 5.7 - 0.47\,(K_p)_{-12} \quad \text{for} \quad K_p < 5 \tag{4}$$

where $(K_p)_{-12}$ is the maximum value of $K_p$ for the 12 preceding hours (Carpenter and Park. 1973). A similar decrease of the post-midnight plasmapause is predicted by the theoretical models when f decreases (see Figures 6 and 7);

ii) early whistlers observations by Carpenter (1966) have shown that during quiet times (i.e. low $K_p$) the plasmapause tends to a more circular shape as is shown in Figures 5 and 6 for $f = 1.3$;

iii) a noon-midnight asymmetry of the plasmasphere has recently been found by Carpenter and Selly (1975) from very quiet time whistler drift paths observations. Gringauz and Bezrukikh (1975) deduced also from PROGNOZ observations that after a long period of low $K_p$ the noon plasmapause is located at significantly larger L values than in the midnight sector. Using McIlwain's electric field model E3H for $f = 1.3$ a similar noon-midnight asymmetry is predicted ;

iv) when magnetic activity increases the noon-midnight asymmetry of the plasmasphere and plasmapause decreases (Gringauz and Bezrukikh, 1975; Carpenter and Selly, 1975). This tendency is also seen in Figures 6 and 7 where L(1200LT) - L(0100LT) decreases when f decreases ;

v) it is known since a long time that the plasmapause has a bulge in the dusk sector during constant moderate and high geomagnetic activity. (Carpenter, 1966). Recently Park (1975)

presented very clear evidence that during moderate substorm activity the whistler paths in the outer plasmasphere move to higher L shells in the afternoon and evening sector from 1600 LT to 2000 LT. This indicates that the equipotential lines in the afternoon-dusk region bulge out toward the 2000 LT direction as predicted by McIlwain's E3H model when the scale factor is less than 1. (see Figure 6). Consequently, the dawn-dusk asymmetry of the plasmapause increases for increasing values of the $K_p$ index and for decreasing values of f.

The qualitative agreements between these (whistler and satellite) observations and our theoretical results can be considered as new arguments for the present theory of plasmapause formation as well as for McIlwain's electric field model EH3 with variable scale factor f. From the present discussion it can also be concluded that the E3H models with large values of f correspond best to the magnetospheric electric field distribution for low $K_p$ index, and conversely the smallest values of f (i.e. f = 0.7 - 0.8) correspond to the larger values of $K_p$.

*APPENDIX*

***A tentative relationship between f and $K_p$***

It has been shown above that McIlwain's (1974) E3H model with a variable scale factor f describes, at least qualitatively, the plasmapause positions as a function of the local time angle and as a function of geomagnetic activity. Therefore it is tempting to relate the scale factor f to the value of the geomagnetic index $K_p$. Such a relation can in principle be deduced from correlated observations of the plasmapause position at a fixed local time, $\varphi$. Equation (4) illustrates such a relationship between the maximum $K_p$ index for the 12 preceeding hours and the observed position of the plasmapause near midnight.

On the other hand, according to the theory, the plasmapause position at 0100 LT is approximately given by the linear relation

$$R_{pp}(0100\ LT) = 1.1 + 3.5\ f \qquad (A1)$$

This relation is illustrated in Figure 7 by the dotted curve. It fits well the theoretical curve (solid line, 0100LT) for $0.75 < f < 1.2$.

Combining equation (4) and (A1), and neglecting the slight difference between the equatorial distance ($R_{pp}$) and McIlwain's parameter ($L_{pp}$) one obtains

$$f = 1.31 - 0.134\,(K_p)_{-12} \qquad (A2)$$

Which is approximately applicable in the range $0 < K_p < 4$ due to the limitations of equations (4) and (A1).

It would be interesting to deduce similar relationships from observations of the plasmapause at other different local time angles, and compare them to (A2). If all these relations $f = f(K_p)$ would be for instance nearly identical we would be able to conclude that the large

scale magnetospheric electric field distribution can be represented very precisely by McIlwain's E3H model and that its change with $K_p$ can actually be described by the variation of *one* single parameter, f. It is however very unlikely that the variation of only one parameter is sufficient to describe the complex changes of the large scale magnetospheric electric field distribution as a function of geomagnetic activity. But such a test would certainly be useful to estimate in which way and how much the actual electric field departs from the model E3H. It would also be interesting to conduct such a test to verify the proposed theory for the plasmapause formation under constant geomagnetic conditions. Unfortunately the magnetic activity is rarely constant for 24 consecutive hours; therefore time dependent models of the magnetospheric electric field and plasma convection must be the next goal of our efforts to describe the detailed plasmapause position as a function of local time and changing magnetic activity conditions.

*ACKNOWLEDGEMENTS*

I want to thank Dr. C.E. McIlwain who provided us with the computer subroutines of his model E3H. It is a pleasure to express my thanks to Professor M. Nicolet for his valuable support during the preparation of this paper. I appreciated the discussion and comments of Drs. A. Nishida, M. Petit, and M. Blanc.

*REFERENCES*


BRIDGE, H., A. EGIDI, A. LAZARUS, E. LYON, and L. JACOBSON, Preliminary results of plasma measurements on IMP-A, *in Space Res.*, 5, 969-978, North-Holland Publ. Co., Amsterdam, 1965.

CARPENTER, D.L., Whistler studies of the plasmapause in the magnetosphere. I. Temporal variations in the position of the knee and some evidence of plasma motions near the knee, *J. Geophys. Res.*, 71, 693-709, 1966.

CARPENTER, D.L. and C.G. PARK, On what ionospheric workers should know about the plasmapause-plasmasphere, *Rev. Geophys. Space Phys.*, 11, 133-154, 1973

CARPENTER, D.L. and N.T. SEELY, Cross-L Plasma drifts in the outer plasmasphere: quiet-time patterns and some substorm effects, (Submitted to J. Geophys. Res.), 1975.

EGIDI, A., V. FORMISANO, F. PALMIOTTO, P. SARACENO, and G. MORENO, Solar wind and location of shock front and magnetopause at 1969 solar maximum, *J. Geophys. Res.*, 75, 6999-7006, 1970.

FAIRFIELD, D.H., Average and unusual locations of the Earth's magnetopause and bow shock, *J. Geophys. Res.*, 76, 6700-6716, 1971.

GRINGAUZ, K.I., and V.V. BEZRUKIKH, Asymmetry of earth's plasmasphere in direction noon-midnight from data of measurements on satellites Prognoz and Prognoz-2, paper presented at Symposium on *Physics of Plasmapause*, Grenoble, Sept. 1975.

GRINGAUZ, K.I., G.N. ZASTENKER, and M.Z. KHOKHLOV, Variations in position of magnetopause from data of charged particle traps on Prognoz and Prognoz-2 Satellites, *Cosmic Research*, 12, 815-818, 1975.

LEMAIRE, J., The "Roche-Limit" of ionospheric plasma and the plasmapause formation, *Planet. Space Sci.*, 22, 757-766, 1974.

LEMAIRE, J., The mechanisms of formation of the Plasmapause, *Ann. Geophys.*, t 31, fasc. 1, 175-190, 1975.

MAUK, B.H., and C.E.McILWAIN,Correlation of Kp with the substorm-injected Plasma Boundary, *Journ. Geophys. Res.*, 22, 3193-3196, 1974.

McILWAIN, C.E., Plasma convection in the vicinity of the geosynchronous orbit, in *"Earth magnetospheric Processes"*, 268-279, ed. B.M. McCormac, D. Reidel Publ. Co., Dordrecht-Holland, 1972.

McILWAIN, C.E., Substorm injection boundaries, *Magnetospheric Physics*, 143-154, ed. B.M. McCormac, D. Reidel Publishing Co., Dordrecht-Holland, 1974.

OLSON, W.P., and K.A. PFITZER, A quantitative model of the magnetospheric magnetic field, *J. Geophys. Res.*, **79**, 3739-3748, 1974.

PARK, C.G., Substorm electric fields in the evening plasmasphere and their effects on the underlying F layer, (submitted to J. Geophys. Res.), 1975.

SONNERUP, B.U.O., and M.J. LAIRD, On magnetospheric interchange instability, *J. Geophys. Res.*, **68**, 131-139, 1963.

100 - BIAUME, F., Détermination de la valeur absolue de l'absorption dans les bandes du système de Schumann-Runge de l'oxygène moléculaire, 1972.

101 - NICOLET, M. and W. PEETERMANS, The production of nitric oxide in the stratosphere by oxidations of nitrous oxide, 1972.

102 - VAN HEMELRIJCK, E. et H. DEBEHOGNE, Observations au Portugal de phénomènes lumineux se rapportant à une expérience de lâcher de barium dans la magnétosphère, 1972.

103 - NICOLET, M. et W. PEETERMANS, On the vertical distribution of carbon monoxide and methane in the stratosphere, 1972.

104 - KOCKARTS, G., Heat balance and thermal conduction, 1972.

105 - ACKERMAN, M. and C. MULLER, Stratospheric methane from infrared spectra, 1972.

106 - ACKERMAN, M. and C. MULLER, Stratospheric nitrogen dioxide from infrared absorption spectra, 1972.

107 - KOCKARTS, G., Absorption par l'oxygène moléculaire dans les bandes de Schumann-Runge, 1972.

108 - LEMAIRE, J. et M. SCHERER, Comportements asymptotiques d'un modèle cinétique du vent solaire, 1972.

109 - LEMAIRE, J. and M. SCHERER, Plasma sheet particle precipitation : A kinetic model, 1972.

110 - BRASSEUR, G. and S. CIESLIK, On the behavior of nitrogen oxides in the stratosphere, 1972.

111 - ACKERMAN, M. and P. SIMON, Rocket measurement of solar fluxes at 1216 Å, 1450 Å and 1710 Å, 1972.

112 - CIESLIK, S. and M. NICOLET, The aeronomic dissociation of nitric oxide, 1973.

113 - BRASSEUR, G. and M. NICOLET, Chemospheric processes of nitric oxide in the mesosphere and stratosphere, 1973.

114 - CIESLIK, S. et C. MULLER, Absorption raie par raie dans la bande fondamentale infrarouge du monoxyde d'azote, 1973.

115 - LEMAIRE, J. and M. SCHERER, Kinetic models of the solar and polar winds, 1973.

116 - NICOLET, M., La biosphère au service de l'atmosphère, 1973.

117 - BIAUME, F., Nitric acid vapor absorption cross section spectrum and its photodissociation in the stratosphere, 1973.

118 - BRASSEUR, G., Chemical kinetic in the stratosphere, 1973.

119 - KOCKARTS, G., Helium in the terrestrial atmosphere, 1973.

120 - ACKERMAN, M., J.C. FONTANELLA, D. FRIMOUT, A. GIRARD, L. GRAMONT, N. LOUISNARD, C. MULLER and D. NEVEJANS, Recent stratospheric spectra of NO and $NO_2$, 1973.

121 - NICOLET, M., An overview of aeronomic processes in the stratosphere and mesosphere, 1973.

122 - LEMAIRE, J., The "Roche-Limit" of ionospheric plasma and the formation of the plasmapause, 1973.

123 - SIMON, P., Balloon measurements of solar fluxes between 1960 Å and 2300 Å, 1974.

124 - ARIJS, E., Effusion of ions through small holes, 1974.

125 - NICOLET, M., Aëronomie, 1974.

126 - SIMON, P., Observation de l'absorption du rayonnement ultraviolet solaire par ballons stratosphériques, 1974.

127 - VERCHEVAL, J., Contribution à l'étude de l'atmosphère terrestre supérieure à partir de l'analyse orbitale des satellites, 1973.

128 - LEMAIRE, J. and M. SCHERER, Exospheric models of the topside ionosphere, 1974.

129 - ACKERMAN, M., Stratospheric water vapor from high resolution infrared spectra, 1974.

130 - ROTH, M., Generalized invariant for a charged particle interacting with a linearly polarized hydromagnetic plane wave, 1974.

131 - BOLIN, R.C., D. FRIMOUT and C.F. LILLIE, Absolute flux measurements in the rocket ultraviolet, 1974.

132 - MAIGNAN, M. et C. MULLER, Méthodes de calcul de spectres stratosphériques d'absorption infrarouge, 1974.

133 - ACKERMAN, M., J.C. FONTANELLA, D. FRIMOUT, A. GIRARD, N. LOUISNARD and C. MULLER, Simultaneous measurements of NO and $NO_2$ in the stratosphere, 1974.

134 - NICOLET, M., On the production of nitric oxide by cosmic rays in the mesosphere and stratosphere, 1974.

135 - LEMAIRE, J. and M. SCHERER, Ionosphere-plasmasheet field aligned currents and parallel electric fields, 1974.

136 - ACKERMAN, M., P. SIMON, U. von ZAHN and U. LAUX, Simultaneous upper air composition measurements by means of UV monochromator and mass spectrometer, 1974.

137 - KOCKARTS, G., Neutral atmosphere modeling, 1974.

138 - BARLIER, F., P. BAUER, C. JAECK, G. THUILLIER and G. KOCKARTS, North-South asymmetries in the thermosphere during the last maximum of the solar cycle, 1974.

139 - ROTH, M., The effects of field aligned ionization models on the electron densities and total flux tubes contents deduced by the method of whistler analysis, 1974.

140 - DA MATA, L., La transition de l'homosphère à l'hétérosphère de l'atmosphère terrestre, 1974.

141 - LEMAIRE, J. and R.J. HOCH, Stable auroral red arcs and their importance for the physics of the plasmapause region, 1975.

142 - ACKERMAN, M., NO, $NO_2$ and $HNO_3$ below 35 km in the atmosphere, 1975.

143 - LEMAIRE, J., The mechanisms of formation of the plasmapause, 1975.

144 - SCIALOM, G., C. TAIEB and G. KOCKARTS, Daytime valley in the F1 region observed by incoherent scatter, 1975.

145 - SIMON, P., Nouvelles mesures de l'ultraviolet solaire dans la stratosphère, 1975.

146 - BRASSEUR, G. et M. BERTIN, Un modèle bi-dimensionnel de la stratosphère, 1975.

147 - LEMAIRE, J. et M. SCHERER, Contribution à l'étude des ions dans l'ionosphère polaire, 1975.

148 - DEBEHOGNE, H. et E. VAN HEMELRIJCK, Etude par étoiles-tests de la réduction des clichés pris au moyen de la caméra de triangulation IAS, 1975.

149 - DEBEHOGNE, H. et E. VAN HEMELRIJCK, Méthode des moindres carrés appliquée à la réduction des clichés astrométriques, 1975.

150 - DEBEHOGNE, H. et E. VAN HEMELRIJCK, Contribution au problème de l'abérration différentielle, 1975.

151 - MULLER, C. and A.J. SAUVAL, The CO fundamental bands in the solar spectrum, 1975.

152 - VERCHEVAL, J., Un effet géomagnétique dans la thermosphère moyenne, 1975.

153 - AMAYENC, P., D. ALCAYDE and G. KOCKARTS, Solar extreme ultraviolet heating and dynamical processes in the mid-latitude thermosphere, 1975.

154 - ARIJS, E. and D. NEVEJANS, A programmable control unit for a balloon borne quadrupole mass spectrometer, 1975.

155 - VERCHEVAL, J., Variations of exospheric temperature and atmospheric composition between 150 and 1100 km in relation to the semi-annual effect, 1975.

156 - NICOLET, M., Stratospheric Ozone : An introduction to its study, 1975.

157 - WEILL, G., J. CHRISTOPHE, C. LIPPENS, M. ACKERMAN and Y. SAHAI, Stratospheric balloon observations of the southern intertropical arc of airglow in the southern american aera, 1976.

158 - ACKERMAN, M., D. FRIMOUT, M. GOTTIGNIES, C. MULLER, Stratospheric HCl from infrared spectra, 1976.

159 - NICOLET, M., Conscience scientifique face à l'environnement atmosphérique, 1976.

160 - KOCKARTS, G., Absorption and photodissociation in the Schumann-Runge bands of molecular oxygen in the terrestrial atmosphere, 1976.